Journal of the Mechanical Behavior of Biomedical Materials 95 (2019) 143–152

Contents lists available at ScienceDirect

Journal of the Mechanical Behavior of Biomedical Materials

journal homepage: www.elsevier.com/locate/jmbbm

Exposure effects of endotoxin-free titanium-based wear particles to human osteoblasts

Bruna C. Costa[a,*], Alexandra C. Alves[b], Fatih Toptan[b,c], Ana M. Pinto[b,c], Liliana Grenho[d,e], Maria H. Fernandes[d,e], Dmitri Y. Petrovykh[f], Luís A. Rocha[g], Paulo N. Lisboa-Filho[g]

[a] Graduate Program in Materials Science and Technology, POSMAT, UNESP, São Paulo State University, 17033-360, Bauru, SP, Brazil
[b] CMEMS-UMinho, Center for Micro Electro Mechanical Systems, University of Minho, 4800-058, Azurém, Portugal
[c] Department of Mechanical Engineering, University of Minho, 4800-058, Azurém, Portugal
[d] Laboratory for Bone Metabolism and Regeneration, Faculty of Dental Medicine, U. Porto, FMDUP, 4200-393, Porto, Portugal
[e] LAQV/REQUIMTE, U. Porto, 4200-393, Porto, Portugal
[f] International Iberian Nanotechnology Laboratory, 4715-330, Braga, Portugal
[g] Department of Physics, UNESP, São Paulo State University, 17033-360, Bauru, SP, Brazil

ARTICLE INFO

Keywords:
Titanium implants
Degradation
Wear particles
Endotoxins
Biological effects

ABSTRACT

Titanium-based materials are widely employed by the biomedical industry in orthopedic and dental implants. However, when placed into the human body, these materials are highly susceptible to degradation processes, such as corrosion, wear, and tribocorrosion. As a consequence, metallic ions or particles (debris) may be released, and although several studies have been conducted in recent years to better understand the effects of their exposure to living cells, a consensual opinion has not yet been obtained. In this work, we produced metallic-based wear particles by tribological tests carried out on Ti-6Al-4V and Ti-15Zr-15Mo alloys. They were posteriorly physicochemically characterized according to their crystal structure, size, morphology, and chemical composition and compared to Ti-6Al-4V commercially available particles. Finally, adsorbed endotoxins were removed (by applying a specific thermal treatment) and endotoxin-free particles were used in cell experiments to evaluate effects of their exposure to human osteoblasts (MG-63 and HOb), namely cell viability/metabolism, proinflammatory cytokine production (IL-6 and PGE2), and susceptibility to internalization processes. Our results indicate that tribologically-obtained wear particles exhibit fundamental differences in terms of size (smaller) and morphology (irregular shapes and rough surfaces) when compared to the commercial ones. Consequently, both Ti-6Al-4V and Ti-15Zr-15Mo particles were able to induce more pronounced effects on cell viability (decrease) and cytokine production (increase) than did Ti-6Al-4V commercial particles. Furthermore, both types of wear particles penetrated osteoblast membranes and were internalized by the cells. Influences on cytokine production by endotoxins were also demonstrated.

1. Introduction

Among the metallic implant biomaterials (Chen and Thouas, 2015), the mechanical properties, biocompatibility, and corrosion resistance of titanium (Ti) and its alloys make them particularly favorable for use in dental (Cordeiro and Barão, 2017) and orthopedic (Geetha et al., 2009) implants. Industrial production of Ti-based biomaterials is dominated by commercially pure titanium (cp-Ti) and a Ti alloy with 6 wt% of aluminum (Al) and 4 wt% of vanadium (V), denoted hereafter as Ti-6Al-4V (Chen and Thouas, 2015; Cordeiro and Barão, 2017). More recently, to address the reported long-term health effects associated with Al and V, new titanium alloys (Gepreel and Niinomi, 2013; Niinomi et al., 2012), such as Ti-15Zr-15Mo with 15 wt% each of zirconium (Zr) and molybdenum (Mo), have been proposed (Correa et al., 2016, 2015; 2014; Xavier et al., 2017).

Many of the beneficial characteristics of Ti-based materials are associated with both passivation and protection provided by the surface film formed on these materials in contact with biological fluids (Sundell et al., 2017; Wang et al., 2016). Nevertheless, over time any implant material is subject to degradation through wear, corrosion, and their synergistic effect known as tribocorrosion (Mathew et al., 2009; Ponthiaux et al., 2012). Consequently, metallic ions and/or particles

* Corresponding author. Graduate Program in Materials Science and Technology, POSMAT, UNESP, São Paulo State University, Av. Eng. Luiz Edmundo Carrijo Coube 14-01, 17033-360, Bauru, SP, Brazil.(Tel.: +55 14 31036000x6481)
E-mail address: b.costa@unesp.br (B.C. Costa).

https://doi.org/10.1016/j.jmbbm.2019.04.003
Received 27 February 2019; Received in revised form 4 April 2019; Accepted 5 April 2019
Available online 10 April 2019
1751-6161/

may be released from the implant surface and affect the surrounding living cells and tissues. However, the associated short and long-term biological effects are still unclear (Alves et al., 2013, 2015; Amanatullah et al., 2016; Cvijović-Alagić et al., 2016; Ribeiro et al., 2016; Vasconcelos et al., 2016).

Common effects associated with the accumulation of wear particles in living organisms include: local fibrosis/necrosis, characterized by a greyish appearance of the tissues surrounding an implant, known as metallosis (C. A. Oliveria et al., 2015; Watters et al., 2010); excessive activation of macrophages; increased production of proinflammatory cytokines, namely the tumor necrosis factor α (TNF- α), interleukins 1, 1α, 1β, 6, and 10 (IL-1, IL-a, IL-1β, IL-6, and IL-10) and prostaglandin E2 (PGE2) (Bitar and Parvizi, 2015; Hallab and Jacobs, 2017; Landgraeber et al., 2014; Sukur et al., 2016; Veronesi et al., 2017) by immune-system cells, bone cells (osteoblasts), and connective tissue cells (fibroblasts), which can activate/stimulate osteoclasts, ultimately leading to the bone resorption and implant loosening by osteolysis (Bitar and Parvizi, 2015; Veronesi et al., 2017); and a pathology known as “particle disease” (Sukur et al., 2016; Vasconcelos et al., 2016).

The specific physicochemical characteristics of the metallic wear particles, e. g., crystallinity, size, morphology, and chemical composition, play an important role in determining their biological effects (Konttinen and Pajarinen, 2013; Li et al., 2014). For retrieved or simulated wear particles, the current literature is primarily focused on two popular orthopedic implant materials: cobalt-chromium alloys (Co-Cr) and ultra-high-molecular-weight polyethylene (UHMWPE) (Afolaranmi et al., 2012; Hongtao et al., 2011; Horev-Azaria et al., 2011; Kwon et al., 2009; Papageorgiou et al., 2008; Pourzal et al., 2011; Sansone et al., 2013; Wang et al., 2010). In contrast, rather than using retrieved or simulated wear particles, most studies of Ti-based implant materials rely on model cp-Ti particles with controlled size and morphology and examine their effects on immune-system cells (macrophages and/or monocytes), connective-tissue cells (fibroblasts), or mesenchymal stem cells (Haleem-Smith et al., 2012; Lee et al., 2012; Mostardi et al., 2010; Soto-Alvaredo et al., 2014; Wu et al., 2008).

Here, we produced simulated-wear particles of Ti-6Al-4V and Ti-15Zr-15Mo from tribological tests under physiological electrolyte conditions. These wear particles were characterized and compared to commercial Ti-6Al-4V particles for crystal structure, chemical composition, size, and morphology. To avoid false positives in the subsequent cell viability and cytokine assays due to the presence of surface-adsorbed endotoxins (residual lipopolysaccharides (LPS) from Gram-negative bacteria, which are not considered in most particle studies) (Li and Boraschi, 2016; Magalhães et al., 2007), all the particles were thermally treated under conditions sufficient to inactivate any adherent endotoxins (Magalhães et al., 2007; McIntyre and Reinin, 2009). Two different cell lines of human osteoblasts were then exposed *in vitro* to the endotoxin-free Ti-based particles to investigate their internalization as well as any effects on cell viability and production of proinflammatory cytokines interleukin 6 (IL-6) and prostaglandin 2 (PGE2).

2. Materials and methods

2.1. Materials

Commercial Ti-6Al-4V discs (20 mm in diameter and 3.5 mm in thickness, from VSMPO TIRUS, USA) and in-house-processed arc-melted Ti-15Zr-15Mo ingot cuts (irregular shapes and 3.5 mm in thickness, from Anelasticity and Biomaterials Laboratory, UNESP—Bauru, Brazil) were used as sources of simulated-wear particles. The crystallographic structures of both bulk materials were characterized by X-ray diffraction (XRD) using a diffractometer (D/MAX 2100 PC, Rigaku) with Cu-Kα source operated at a voltage of 40 kV and current of 20 mA, divergence slit of 1°, receiving slit of 0.3 mm, a nickel filter, and a 10–100° XRD angular scan with 0.02° steps at 1.6 s per step. The microstructure and chemical composition of the bulk alloys were characterized by scanning electron microscopy (SEM) in a commercial microscope (EVO LS15, Carl Zeiss) equipped with an energy-dispersive spectroscopy (EDS) detector (Inca ACT-X, Oxford). Commercial Ti-6Al-4V particles were purchased from Electro-Optical Systems, USA.

2.2. Production and characterization of wear particles

Wear particles of Ti-6Al-4V or Ti-15Zr-15Mo were produced by tribological experiments in a pin-on-disc tribometer operated in reciprocating mode, using an alumina ball (10 mm in diameter) as a counter-body. Before tests, all samples were gradually polished down to #1200 grade SiC paper, cleaned in an ultrasonic bath, alternating deionized water and ethanol as cleaning solutions, etched 30 s in a 1:1:1 (by volume) mixture of phosphoric acid (H_3PO_4), hydrochloric acid (HCl), and deionized water (H_2O), and cleaned again in an ultrasonic bath. A fresh phosphate-buffered saline (PBS) solution was prepared for each experiment by dissolving sodium chloride (NaCl, 8 g/L), potassium chloride (KCl, 0.2 g/L), disodium phosphate (Na_2HPO_4, 1.44 g/L), and monopotassium phosphate (KH_2PO_4, 0.24 g/L) in deionized water. Using the fresh PBS as an electrolyte simulating physiological fluid, several multi-hour tribological experiments were performed under the following conditions: a normal load of 3 N, frequency of 1 Hz, and electrolyte temperature of 37 ± 2 °C (body temperature).

At the end of each tribological experiment, wear particles of Ti-6Al-4V or Ti-15Zr-15Mo were collected, stored in falcon tubes, separated from electrolyte by centrifugation and dried at room temperature. The size, morphology, and chemical composition of the collected wear particles and the commercial Ti-6Al-4V particles were characterized by SEM in a commercial microscope (Quanta 650, FEI) equipped with an energy-dispersive spectroscopy (EDS) detector (Inca ACT-X, Oxford). The crystal structure of the particles was characterized by electron diffraction in a transmission electron microscope (TEM, JEM-2100, JEOL) operated at an accelerating voltage of 200 kV.

2.3. Endotoxin removal

To remove/inactivate any adherent endotoxins, thermal treatments were applied to the commercial Ti-6Al-4V particles and the wear particles of Ti-6Al-4V and Ti-15Zr-15Mo in a thermogravimetric and differential scanning calorimeter (TGA/DSC) system (1 STAR, Mettler-Toledo) equipped with a gas analysis system (OmniStar GSD320, Pfeiffer Vacuum). Following the literature recommendation of treatment at 250 °C for > 30 min (Magalhães et al., 2007; McIntyre and Reinin, 2009), the particles were treated at 250 °C for 45 min, under Ar gas flow (50 mL/min) to avoid thermal oxidation. The heat-treated particles were evaluated for the presence of any residual active endotoxin by Limulus amoebocyte lysate (LAL) gel-clot assays with sensitivities of 0.06 EU/mL and 0.125 EU/mL (ToxinSensor Single Test Kits, GenScript), according to the manufacturer recommendations.

Briefly, LAL assays provide - qualitative and semi-quantitative information regarding the presence of endotoxins in a sample by the reaction with a specific enzyme (amoebocyte) from the *Limulus Polyphemus* horseshoe crab's blood (tested samples are mixed with enzyme aliquots at the bottom of endotoxin-free test tubes). When the amount of adsorbed endotoxins in a sample is higher than the test sensitivity, a positive reaction occurs and a firm clot is observed at the bottom of the test tubes, remaining in place when they are inverted upside down.

To perform the LAL tests, positive controls (C1 and C2) were prepared from the total content reconstitution of the Control Standard for Endotoxin vial (CSE, GenScript, 15 EU) in 1 mL of endotoxin-free water (Lonza EU/mL < 0.005), followed by vortex mixing for 15 min for complete homogenization. Then, the initial positive control (15 EU/mL) was serially diluted for final concentrations of C1 = 0.250 EU/mL and C2 = 0.125 EU/mL. Finally, after heat treatments, all particle samples were dispersed in endotoxin-free PBS (EU/mL < 0.01) at

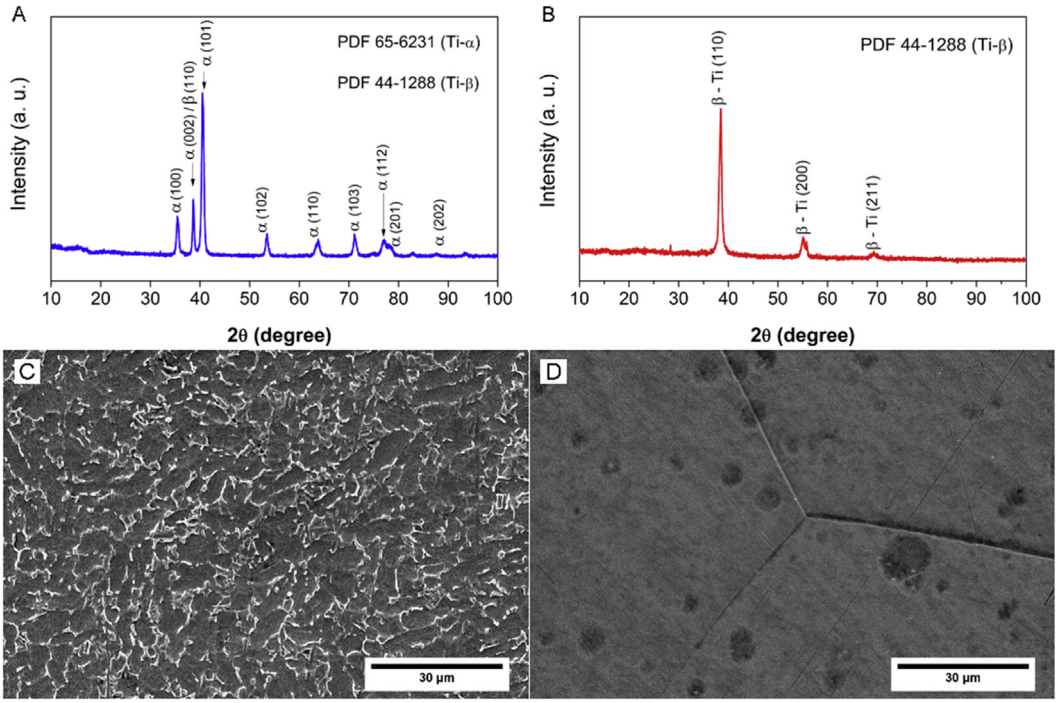

Fig. 1. Bulk crystal structure and surface microstructure of Ti alloys used to generate wear particles. XRD wide-angle scans and SEM images are shown for the commercial Ti-6Al-4V alloy (A and C) and in-house-processed Ti-15Zr-15Mo alloy (B and D).

concentrations of 500 and 100 μg/mL (ten-fold higher than those posteriorly used in cell experiments). All dispersions were used for the LAL gel-clot assays that were compared to the positive controls C1 and C2, regarding the clotting reaction.

2.4. Cell-viability assays

Osteoblast-like cells (MG63, ATCC) and primary normal human osteoblasts (HOb, Sigma-Aldrich) were cultured at 37 °C in a 5% CO_2 atmosphere, respectively, in α-MEM and Growth Media (both from Sigma-Aldrich) cell-culture media, supplemented with 10% ultra-low-endotoxin fetal bovine serum (FBS, Biowest), 1% of penicillin/streptomycin, and 1% of amphotericin B.

For cell-viability assays, 3×10^3 cells were cultured in the wells of a 96-well plate and incubated for 24 h at 37 °C in a 5% CO_2 atmosphere. Taking advantage of its accelerated proliferation rate, an initial dose-response survey was performed with MG63 cell line for particle concentrations of 100, 50, 10, 1, 0.5, and 0.1 μg/mL and experimental periods of 1, 2, 3, and 7 days. Based on the results obtained for MG63 cell line and values reported in the literature for possible *in vivo* metal concentrations in patients with a titanium prosthesis (Hallab et al., 2001), particle concentrations of 50 and 10 μg/mL and experimental periods of 3 and 7 days were chosen for the cell-viability assays for HOb cell line.

For both MG63 and HOb cell lines, all cell-viability assays were conducted in triplicate and the untreated control group consisted of cells cultured only in the supplemented cell culture medium, as specified above. Cell viability was assessed by 3-(4,5-dimethylthiazol-2-yl)-2,5-diphenyltetrazolium bromide (MTT) reduction staining test. After the specified incubation periods, 100 μL of MTT (0.5 mg/mL) was added to each well and the culture plates were incubated at 37 °C for 4 h. Then, MTT solution was removed, and 50 μL of dimethyl sulfoxide (DMSO) was added to each well. After 30 min, the optical density was measured at 550 nm in a monochromator-based multi-mode microplate reader (Synergy H1, Bio-Tek).

2.5. Particle internalization

The possible particle internalization by HOb cells exposed to the wear particles was investigated by transmission electron microscopy (TEM). In a well of a 24-well plate, 2×10^4 cells/mL were cultured at 37 °C in a 5% CO_2 atmosphere and then exposed to 50 μg/mL of wear particles of Ti-6Al-4V or Ti-15Zr-15Mo for 24 h. The positive control group consisted of cells cultured only in the supplemented cell culture medium, as specified before (see 2.4 Cell-viability assays). After exposure to the wear particles, cells were detached from the plates by trypsinization (0.04% trypsin in 0.25% EDTA solution, 5 min) and centrifuged. The cell pellet was washed in 0.1 M sodium cacodylate buffer, fixed (2.5% glutaraldehyde, 2 h), and post-fixed (2% osmium tetroxide, overnight). Dehydration was performed in graded ethanol solutions and samples were embedded in epoxy resin (EPON, Hexion). Ultra-thin (100 nm) sections were prepared in a RMC Ultramicrotome (PowerTome) using a diamond knife and mounted on copper grids. Finally, grids were contrasted with uranyl acetate and lead citrate for TEM analysis at an accelerating voltage of 60 kV (EM 10A, Carl Zeiss).

2.6. Pro-inflammatory cytokine assays

The production of IL-6 and PGE2 cytokines by HOb cells after exposure to wear particles of Ti-6Al-4V or Ti-15Zr-15Mo was evaluated using commercial enzyme-linked immunosorbent assays (ELISA): IL-6 Human ELISA and PGE2 Human ELISA kits, both from Novex. Cell-culture supernatants of HOb cells (see 2.4 Cell-viability assays) exposed to wear particles at the chosen concentrations (50 and 10 μg/mL) and experimental periods (3 and 7 days) were used, according to the manufacturer protocol. The untreated control group consisted of cells cultured only in the supplemented cell culture medium, as specified before (see 2.4 Cell-viability assays). Two additional experimental groups, exposed to endotoxins at 50 or 100 ng/mL (corresponding to 500 and 1,000 EU/mL) prepared from control standard endotoxin (CSE, 15 EU/mL, GenScript), were included. Assays for each set of conditions were conducted in triplicate.

Table 1
Composition of Ti-6Al-4V and Ti-15Zr-15Mo alloys determined by EDS.

Sample	Alloying Elements (wt%)				
	Ti	Al	V	Zr	Mo
Ti-6Al-4V	89.6 ± 0.5	6.4 ± 0.3	4.4 ± 0.6	-	-
Ti-15Zr-15Mo	68.5 ± 0.2	-	-	15.8 ± 0.2	15.7 ± 0.1

2.7. Statistical analysis

Analysis of variance (ANOVA), followed by post-hoc Tukey test in Origin 7.0 software (OriginLab) was conducted to calculate the differences within the datasets ($n = 3$) obtained from MTT and ELISA measurements; p-values < 0.05 were considered statistically significant.

3. Results

3.1. Bulk structure and composition of Ti alloys

Before tribological experiments, the crystal structure and chemical composition of the polished and cleaned bulk samples of Ti alloys were characterized by XRD, SEM, and EDS (Fig. 1, Table 1).

The EDS analysis confirmed the nominal alloying composition for both Ti-6Al-4V and Ti-15Zr-15Mo (Table 1). The commercial Ti-6Al-4V alloy exhibited XRD peaks (Fig. 1A) of hexagonal (α-Ti) crystal structure (ICDD PDF card 65–6231) with a small contribution from a body-centered cubic (β-Ti) crystal structure (ICDD PDF card 44–1288), in agreement with observing β-phase precipitates in an α-Ti matrix by SEM (Fig. 1C). In contrast, the crystal structure of the in-house-processed Ti-15Zr-15Mo alloy is indexed as pure β-Ti (Fig. 1B), and its surface exhibits a characteristic granular β-phase microstructure in SEM images (Fig. 1D).

3.2. Physicochemical characterization of Ti-based particles

Morphology, crystal structure, and chemical composition were investigated for three types of Ti-based particles: wear particles produced from tribological tests on Ti-6Al-4V and Ti-15Zr-15Mo alloys and commercial Ti-6Al-4V particles used as a reference material.

According the obtained results, commercial Ti-6Al-4V particles differ significantly from both types of wear particles. SEM images (Fig. 2A and B) clearly illustrate that these particles have smooth surfaces and an approximately spherical morphology with an average diameter in the 30–45 μm range (Fig. 3A). Both crystal structure and composition of these particles are similar to the characteristics of the commercial bulk Ti-6Al-4V alloy summarized in Fig. 1A and Table 1, with XRD peaks related to the α-Ti and β- Ti phases (Fig. 4A) and close-to-nominal composition determined by EDS: 90.1 ± 1.4 wt% of Ti, 5.5 ± 1.9 wt% of Al, and 4.3 ± 1.5 wt% of V.

In contrast to the commercial Ti-6Al-4V particles, the wear particles of Ti-6Al-4V exhibit rough surfaces and a highly irregular morphology (Fig. 2C and D) with average sizes in the 2–4 μm range (Fig. 3B). Their crystal structure determined by electron diffraction (ED) matches that of the parent material, i.e., the contribution of both α and β-Ti phases (Fig. 4B). The alloying composition of these wear particles was slightly Ti-rich compared to the parent material, with 4.3 ± 0.9 wt% of Al and 3.7 ± 1.4 wt% of V (*cf.* Table 1).

The wear particles of Ti-15Zr-15Mo also exhibit rough surfaces and a highly irregular morphology (Fig. 2E and F), but with average sizes in the 0.6–1.5 μm range (Fig. 3C), which is significantly smaller than those of the Ti-6Al-4V wear particles (*cf.* Fig. 3B) and commercial Ti-6Al-4V particles. Compared to the parent material, the Ti-15Zr-15Mo wear particles follow the same trend as do the Ti-6Al-4V ones, with the ED pattern indexed as β-Ti crystal structure (Fig. 4C) and similar alloying composition (13.3 ± 1.4 wt% of Zr and 13.2 ± 1.1 wt% of Mo, *cf.* Table 1).

3.3. Producing endotoxin-free particles

Surface contamination by endotoxins is notoriously difficult to avoid or remove, due in part to the stability of LPS molecules under conventional autoclave conditions (Li and Boraschi, 2016; Magalhães et al., 2007). Accordingly, to remove or inactivate any adherent endotoxins, all particles were thermally treated at 250 °C for 45 min (Magalhães et al., 2007; McIntyre and Reinin, 2009). After the thermal treatment, each of the three particle types (Ti-6Al4V and Ti-15Zr-15Mo wear particles and commercial Ti-6Al4V particles) was tested at two concentrations (100 and 500 μg/mL, i.e., ten times higher than the chosen concentrations for cell viability and cytokine assays) in LAL gel-clot assays at two sensitivity levels (0.06 and 0.125 EU/mL). Negative results, i.e., no clots for dispersed particle samples in PBS were observed (when compared to the positive controls, which exhibited clot formation when C1 and C2 endotoxin controls were used) for all the LAL gel-clot assays, confirming that all particles, at concentrations used in the subsequent cell experiments, could be designated as endotoxin-free.

3.4. Effects of exposure to Ti-based particles on cell viability

Taking advantage of their high proliferation rate, MG-63 cells were used to test (via MTT assays) the effects on cell viability of exposure to all three of the particle types across a broad range of particle concentrations and experimental periods (Fig. 5). Compared to the untreated controls, exposure to any of the tested particles clearly decreased cell viability, with the strongest effect observed for the Ti-15Zr-15Mo wear particles.

For the more logistically complicated tests with HOb cells, a subset of values for particle concentrations and experimental time points was chosen, informed by the results obtained in the more comprehensive tests with MG-63 cells and previous values reported in the literature (Hallab et al., 2001). Compared to the untreated controls, only exposure to the wear particles significantly decreased the viability of HOb cells, with the strongest effect obtained for the Ti-6Al-4V wear particles (Fig. 6). Complementary evidence from TEM images strongly indicated that upon exposure at 50 μg/mL concentration, both Ti-6Al-4V and Ti-15Zr-15Mo wear particles could be internalized by HOb cells (Fig. 7). Specifically, the observed interaction between particles and the HOb cell membrane indicated the beginning of the internalization process in Fig. 7C and E; already internalized particles can be clearly observed in Fig. 7D and F. The identification of the normal cell structures, such as well-defined cell membrane and nucleus, was confirmed by comparison to the images of the untreated controls (Fig. 7A and B), while the difference between the dark features in the untreated cells and the ones identified as wear particles in Fig. 7C–F was verified by EDS (data not shown).

3.5. Effects of exposure to Ti-based particles on cytokine production

The production of two important proinflammatory cytokines, IL-6 and PGE2, by HOb cells was evaluated by ELISA as a function of exposure to commercial Ti-6Al-4V particles and wear particles of Ti-6Al-4V or Ti-15Zr-15Mo (Fig. 8). Major differences were observed as a function of multiple parameters. For IL-6 production, only the exposure to wear particles for 7 days produced a significant increase compared to the untreated control. A similar IL-6 increase in the endotoxin-exposed controls validated the importance of using endotoxin-free particles in these tests. The PGE2 production exhibited a different pattern, but ultimately became elevated after exposure for 3 days to the highest concentration of both wear particles. The lack of increase in production of either IL-6 or PGE2 upon exposure to the commercial Ti-6Al-4V particles was another notable result of these experiments, highlighting

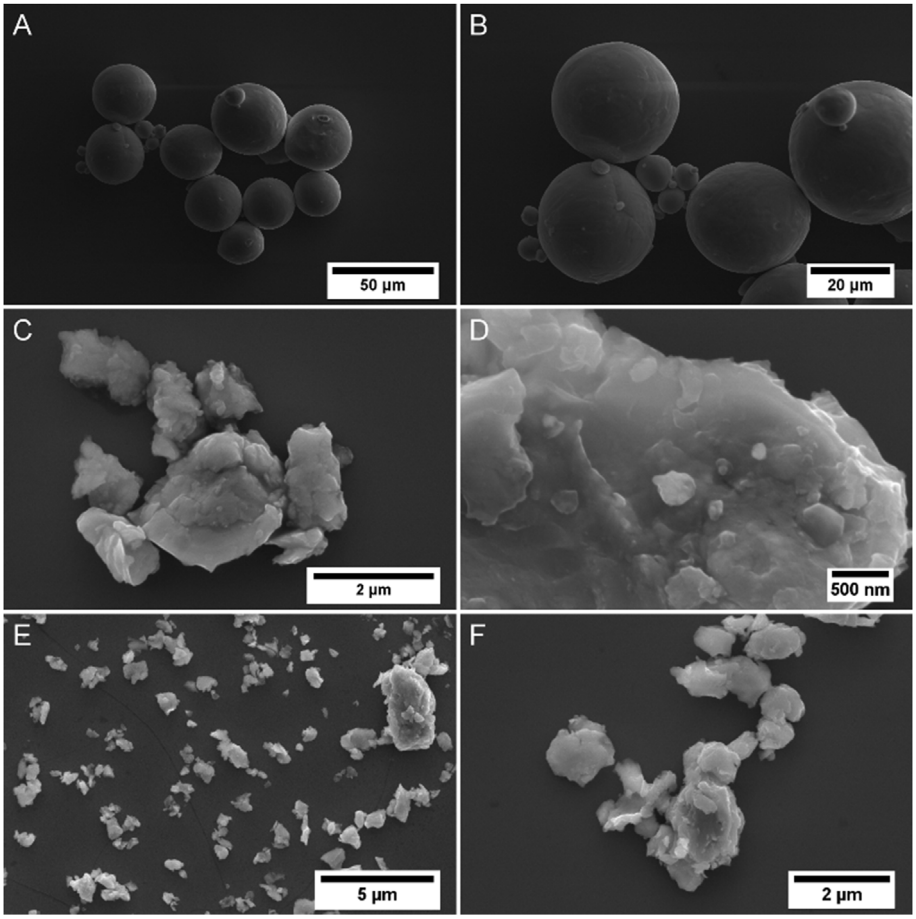

Fig. 2. Size and morphology of Ti-based particles used in experiments with cells. Representative SEM images of commercial Ti-6Al-4V particles (A and B) and of wear particles of Ti-6Al-4V (C and D) and Ti-15Zr15Mo (E and F) produced in tribological experiments.

the critical role of matching not only the crystal structure and composition but also the size and morphology of the wear particles that may be generated *in vivo*.

4. Discussion

Fundamental differences were found in crystal structure and microstructure of Ti-alloys used in tribological tests for wear particle production (Fig. 1). These differences may be attributed to type and number of alloying elements introduced into titanium. Considering the most established Ti-alloy for biomedical purposes, Ti-6Al-4V, the alloying elements aluminum and vanadium were originally introduced into the titanium matrix to improve production costs and mechanical properties when compared to cp-Ti (Cordeiro and Barão, 2017). For the recently proposed Ti-alloys, such as Ti-15Zr-15Mo, it has been reported that the addition of high amounts ($\geq$15 wt%) of β-stabilizing elements, such as molybdenum, allows to obtain a decreased Young's modulus (75 GPa) (Correa et al., 2014) and increased microhardness (400 HV) (Xavier et al., 2017), making these alloys more suitable for bone substitute implants than Ti-6Al-4V (Young's modulus ≈ 110 GPa (Chen and Thouas, 2015) and microhardness ≈ 330 HV (Rocha et al., 2006)).

Usually, harder alloys have higher wear resistance than softer ones (Hacisalihoglu et al., 2015; Perumal et al., 2014). However, the amount of obtained wear particles from tribological tests performed in identical conditions was much higher on Ti-15Zr-15Mo system when compared to Ti-6Al-4V, even though Ti-15Zr-15Mo has a higher measured microhardness value, suggesting that different wear mechanisms are acting on these two Ti-alloys. Thus, besides differences in terms of quantity, the obtained wear particles could also exhibit different physicochemical properties.

Both types of wear particles (Ti-6Al-4V and Ti-15Zr-15Mo) exhibited an irregular morphology and rougher surfaces than did Ti-6Al-4V commercial particles (Fig. 2). These different characteristics may be attributed to their generation mechanism by the sliding process over the parent material during tribological tests. When sliding starts, the surface of the alloys is readily worn out, literally ripping out small particles with irregular shapes and surfaces. Therefore, in this process, it is impossible to control or predict the amount, morphology, and surface characteristics for the generated wear products.

The sizes of Ti-6Al-4V wear particles were, on average, 10 times smaller than those of Ti-6Al-4V commercial particles, while Ti-15Zr-15Mo wear particles were approximately twice and 30 times smaller than Ti-6Al-4V wear particles and Ti-6Al-4V commercial particles, respectively (Fig. 3). Considering the differences in *bulk* mechanical properties and wear mechanisms acting on both titanium alloys during tribological tests and the higher amount of particles produced by Ti-15Zr-15Mo, it is very likely that the earlier produced wear particles left on the worn area interfere in the way that the counter-body further interact with the metal surface, possibly magnifying the wear effects, releasing more particles or fracturing the existing ones (Oliveira et al., 2015).

Regarding physicochemical properties, Ti-6Al-4V and Ti-15Zr-15Mo wear particles were able to maintain the characteristics of the parent material, both in terms of crystal structure (Fig. 4) and chemical composition (Table 1), indicating that, even when these materials are submitted to stressful tribological testing conditions, these bulk characteristics are not altered.

Several studies involving different types of implant-derived wear

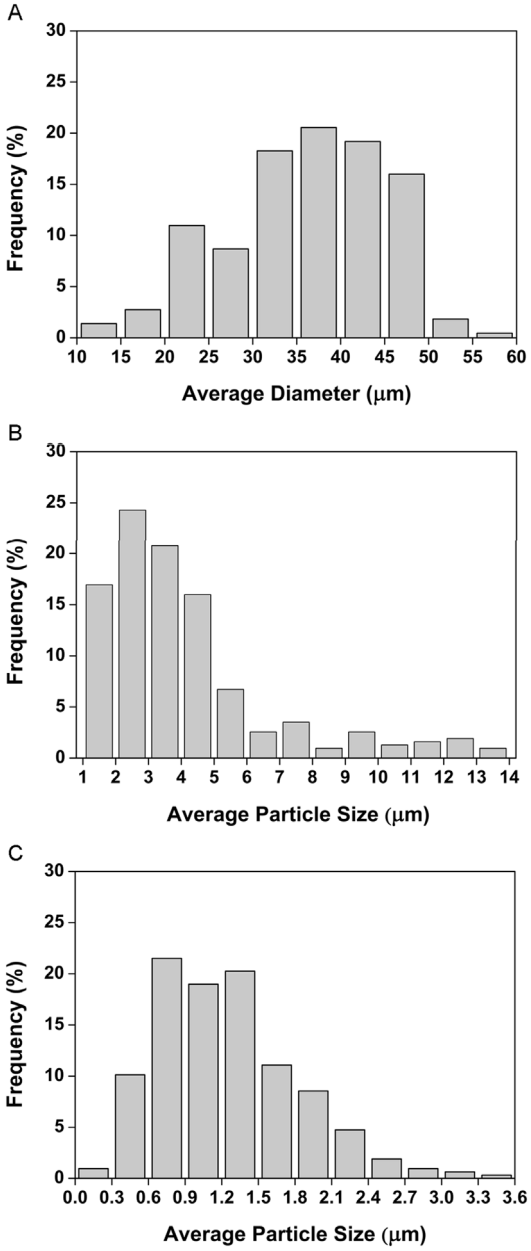

Fig. 3. Particle size distributions determined from SEM images of commercial Ti-6Al-4V particles (A) and wear particles of Ti-6Al-4V (B) and Ti-15Zr-15Mo (C) alloys.

products (ions/particles) and their biological effects on living cells have been conducted recently (Alves et al., 2013, 2015; Amanatullah et al., 2016; Bitar and Parvizi, 2015; Cvijović-Alagić et al., 2016; Konttinen and Pajarinen, 2013; Ribeiro et al., 2016; Sukur et al., 2016; Vasconcelos et al., 2016). Previously, Hallab et al. (2001) already studied the metal concentrations in blood serum and implant-surrounding tissues after revision surgeries in human patients with orthopedic devices based on Ti-6Al-4V alloy (and others). According to their results, titanium (Ti) concentrations about 20% and 60% higher (part per billion, ppb or ng/mL) were found in the blood of patients with Ti-6Al-4V total knee and hip replacements, respectively, and properly functioning, compared to patients without metallic prosthesis. For patients whose total knee and hip replacements were presenting malfunctioning and/or needing revision, titanium concentrations may actually go up to 200% and 5000%, respectively. Besides that, in joint capsules, Ti concentrations may be more than 2 and 250 times higher in patients with

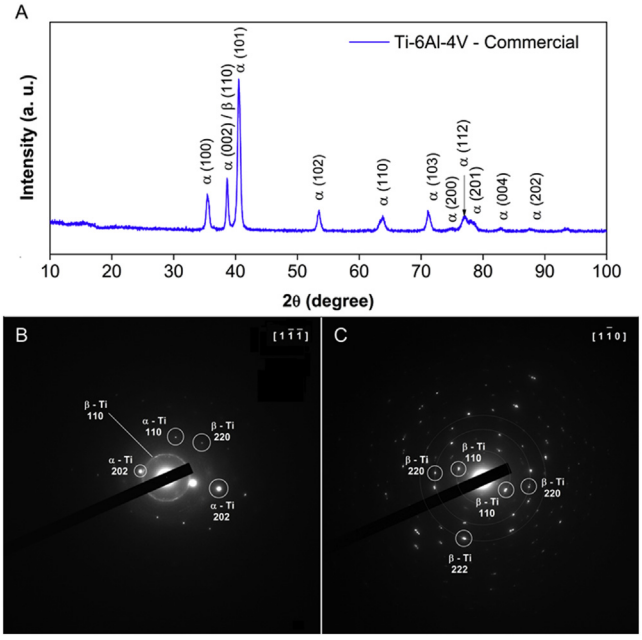

Fig. 4. Crystal structure of Ti-based particles used in experiments with cells. XRD wide-angle scan for commercial Ti-6Al-4V particles (A) and ED patterns for wear particles of Ti-6Al-4V (B) and Ti-15Zr-15Mo (C) alloys.

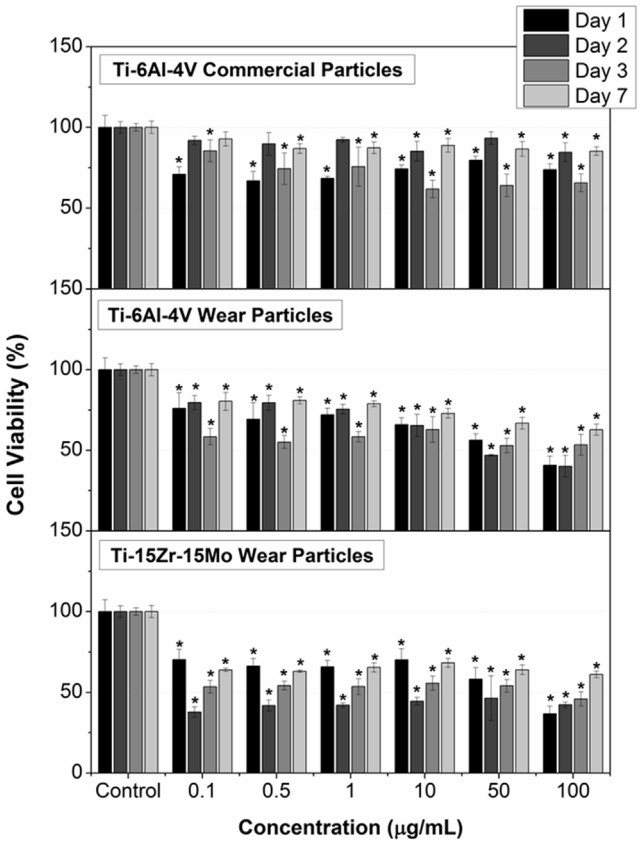

Fig. 5. Viability of MG-63 cells as a function of exposure to commercial Ti-6Al-4V particles and wear particles of Ti-6Al-4V or Ti-15Zr-15Mo. The untreated control cells were cultured in the same medium but without added particles. Asterisk indicates a statistically significant difference from the corresponding control, $p < 0.05$. Particle concentrations are indicated on the bottom axis; grey-scale of the bars corresponds to the duration of exposure. Absorbance values in MTT assays are positively correlated with the number and mitochondrial activity of viable cells in the sample.

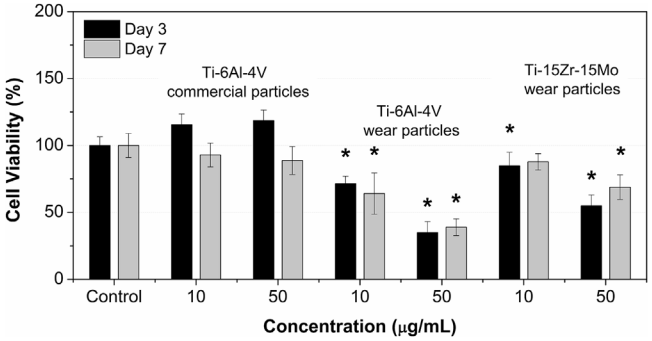

Fig. 6. Viability of HOb cells as a function of exposure to commercial Ti-6Al-4V particles and wear particles of Ti-6Al-4V or Ti-15Zr-15Mo. The untreated control cells were cultured in the same medium but without added particles. Asterisk indicates a statistically significant difference from the corresponding control, $p < 0.05$.

prosthetic devices working properly and malfunctioning, respectively, when compared with prosthetic-free patients. Finally, considering living organs, such as spleen and liver, Ti concentrations may be almost 18 and 80-fold higher (Hallab et al., 2001). These findings indicate a chronic and continuous exposure to metallic compounds (such as titanium) derived from prosthetic devices to the patients' organism.

As previously mentioned, wear particles also may trigger increased production of proinflammatory cytokines by different cells *in vivo*, activating osteoclasts, increasing bone resorption by osteolysis, leading to different adverse tissue reactions, such as metallosis, particle disease and, ultimately, the implant loosening (Amanatullah et al., 2016; Bitar and Parvizi, 2015; Hallab and Jacobs, 2017; Landgraeber et al., 2014; Sukur et al., 2016; Veronesi et al., 2017). Important aspects addressed in these studies are the physicochemical characteristics of the wear particles used, such as, size, morphology, and chemical composition, which will strongly influence their biological fate inside a living organism (Madejczyk et al., 2015; Ribeiro et al., 2016; Sansone et al., 2013; Vasconcelos et al., 2016; Zhang et al., 2017).

Most of the published papers, however, report physicochemical properties and biological effects associated with cobalt-chromium, polyethylene (Afolaranmi et al., 2012; Hongtao et al., 2011; Horev-Azaria et al., 2011; Kwon et al., 2009; Papageorgiou et al., 2008; Pourzal et al., 2011; Sansone et al., 2013; Wang et al., 2010), and commercially available pure titanium-based wear particles, mainly regarding immune-system cells (macrophages) (Haleem-Smith et al., 2012; Lee et al., 2012; Mostardi et al., 2010; Soto-Alvaredo et al., 2014; Wu et al., 2008), wherein commercial particles are commonly used to

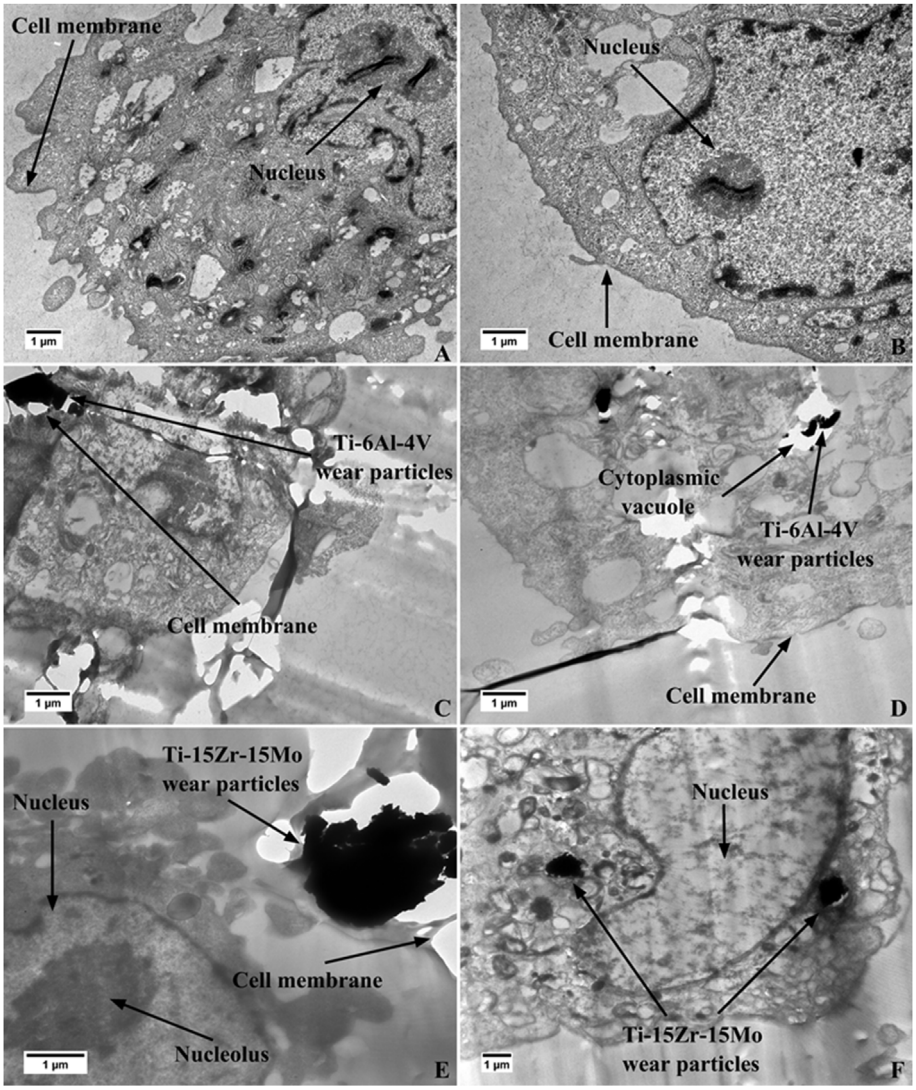

Fig. 7. Ultra-microstructure of HOb cells exposed to Ti-based wear particles. TEM images of the untreated controls (A and B) show well defined and preserved cellular structures. Interacting and internalized wear particles of Ti-6Al-4V, respectively, are indicated in (C) and (D), of Ti-15Zr-15Mo—in (E) and (F).

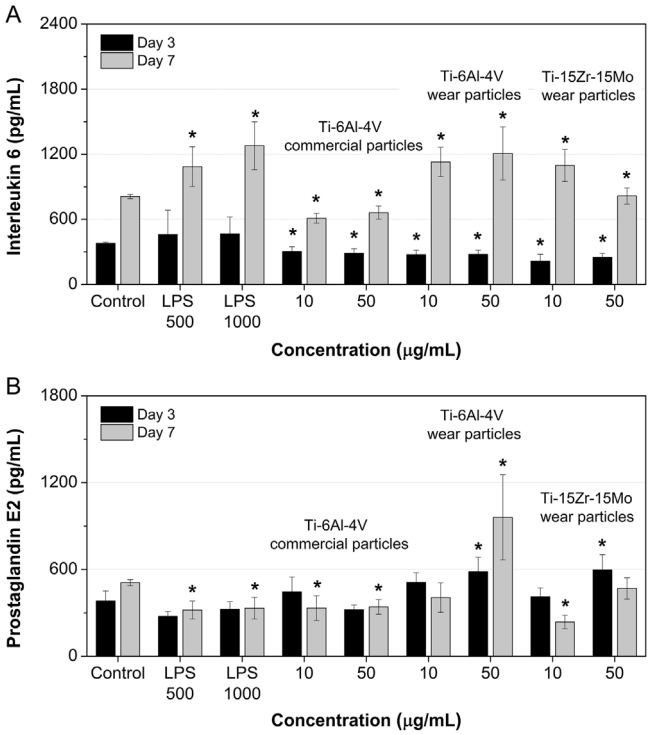

Fig. 8. Cytokine production by HOb cells as a function of exposure to commercial Ti-6Al-4V particles and wear particles of Ti-6Al-4V or Ti-15Zr-15Mo. ELISA results are shown for (A) interleukin 6 (IL-6) and (B) prostaglandin E2 (PGE2). The untreated control cells were cultured in the same medium but without added particles. The endotoxin (LPS) controls were exposed to 500 or 1000 EU/mL of endotoxin. Asterisk indicates a statistically significant difference from the corresponding untreated control, $p < 0.05$.

mimic chemical composition of wear particles. Nevertheless, commercially available particles have controlled sizes and morphologies, significantly differing from what we observed for the wear particles derived from tribological tests as well as for biological effects associated with them and evaluated in the present work (Figs. 5, Figs. 6 and 7).

Another important issue commonly not considered in the literature, is the presence of organic molecules derived from the outer membrane of Gram-negative bacteria, known as endotoxins or lipopolysaccharides (LPS), adsorbed onto the particles. However, since these molecules may trigger effects similar to those associated with wear particles *in vivo*, namely the increased proinflammatory cytokine production, they should be considered before carrying out assays with cells. According to the LAL gel-clot assays performed in this work, all particles used in the subsequent cell experiments may be considered endotoxin-free.

In our cell experiments (Figs. 5, Figs. 6 and 7), we noticed that Ti-6Al-4V commercial particles did not exert strong negative effects on the viability of human osteoblasts, irrespective of the exposure time, particle concentration, or cell line. On the other hand, the exposure to Ti-6Al-4V wear particles (despite their very similar chemical composition) or to Ti-15Zr-15Mo wear particles was able to decrease viability of both MG-63 and HOb cells, for all experimental periods and tested concentrations. Furthermore, both types of wear particles were susceptible to internalization by penetrating across HOb cell membranes, at concentration of 50 μg/mL.

Summarizing the above-mentioned findings, it is possible to conclude that (*i*) considering other physicochemical properties besides chemical composition is extremely important when studying biological effects associated with wear particles; (*ii*) their improved mechanical properties when compared to Ti-6Al-4V notwithstanding, biological effects associated with wear particles generated from new aluminum- and vanadium-free Ti-alloys should be carefully investigated; and (*iii*) not only nanoparticles are susceptible to internalization by living cells, but also those at the microscale, probably due to the ions and proteins adsorption around them, masking their real composition by creating a bio-corona. Once internalized, both micro- and nanosized particles may affect both metabolism of cells and organelles and their protein production (Monopoli et al., 2011; Pederzoli et al., 2017).

Significant differences between results obtained for commercial particles and wear particles were also recorded regarding the evaluation of proinflammatory cytokine production (Fig. 8). Endotoxin-free wear particles are noticeably more liable to induce increased cytokine production, namely IL-6 and PGE2, by HOb cells than are endotoxin-free commercial Ti-6Al-4V particles. The latter presented similar or lower levels of IL-6 and PGE2 production when compared to the positive control, indicating that proinflammatory cytokine production was not promoted by the interaction between the HOb cells and the commercial particles. On the other hand, wear particles of both chemical compositions induced an increased production for both IL-6 and PGE2 by these cells, indicating once more that not only the chemical composition appears to have a strong influence on the way these particles interact with cells, since particles with same compositions but different sizes and morphologies, such as Ti-6Al-4V commercial and wear particles, produced different impacts, probably because the increased ion release rate due to reduced size and/or internalization effect of the wear particles were able to enhance their negative effects. Furthermore, these results also emphasize that both endotoxin-free wear particles and endotoxin positive controls are able to induce increased production of proinflammatory cytokines by osteoblasts, highlighting that endotoxins must not be overlooked in studies of the particle effects.

Taking together the MTT (Fig. 6) and ELISA (Fig. 8) results, an alternative understanding regarding the effects of Ti-based wear particles exposure to human osteoblasts also may be hypothesized. In this work, HOb cell viability was assessed by MTT assays, wherein the cell mitochondrial activity is estimated by absorbance readings of MTT conversion into its formazan product (Kumar et al., 2018). Accordingly, the lower the absorbance reading is correlated with the lower mitochondrial activity, and consequently, the lower cell viability. However, during differentiation processes, osteoblasts may also reduce their aerobic energetic metabolism, and consequently their mitochondrial activity, increasing the expression of specific markers, such as the interleukin-6 (IL-6) production (Peruzzi et al., 2012). Since we verified lower absorbance readings (decreased cell viability) in MTT assays (Fig. 6) and an increased production of IL-6 by HOb cells exposed to Ti-6Al-4V and Ti-15Zr-15Mo wear particles (Fig. 8), mainly at concentration of 50 μg/mL, it is also possible that the interaction of both types of wear particles with the human osteoblasts may have induced their differentiation, as previously reported by others (Bezerra et al., 2017; Fernandes et al., 2018; Rossi et al., 2017).

5. Conclusion

Based on the obtained results, we are able to state that tribologically-obtained Ti-based wear particles (Ti-6Al-4V and Ti-15Zr-15Mo) are significantly different from the commercial ones (Ti-6Al-4V), mainly in terms of sizes (smaller) and morphology (irregular shapes and rough surfaces), such differences being associated with the wear mechanisms acting on the parent materials during tribological tests. Consequently, due to their different physicochemical properties, Ti-6Al-4V and Ti-15Zr-15Mo wear particles also exert different influences on human osteoblasts: more pronounced effects on decreasing cell viability and/or metabolism and on increasing the proinflammatory cytokine production by these cells when compared to the effects of commercial Ti-6Al-4V particles. Ti-based wear particles also exhibited capability to penetrate osteoblast cell membranes and to become internalized. In general, the observed differences between wear particles and commercial particles regarding their biological effects on human osteoblasts may be attributed to the reduced size and increased ion release rate

associated with Ti-6Al-4V and Ti-15Zr-15Mo wear particles, highlighting the importance of considering other characteristics besides chemical composition (the only characteristic commonly mimicked by model particles used in most published studies). Finally, the importance of removing adsorbed endotoxins in studies evaluating biological effects associated with wear particles was also demonstrated.

Funding

This work was supported by Fundação de Amparo à Pesquisa do Estado de São Paulo - FAPESP (2015/50280-5 and 2017/24300-4), Fundação para a Ciência e Tecnologia - FCT (UID/EEA/04436/2013), Coordenação de Aperfeiçoamento de Pessoal de Nível Superior - CAPES (Finance Code 0001), FCT/CAPES Joint Research Project (99999.008666/2014-08), FCT COMPETE 2020 (POCI-01-0145-FEDER-006941 and POCI-01–0145-FEDER-007265) and M-ERA-NET (0001/2015).

Acknowledgements

The authors thank Professor Carlos Roberto Grandini and MSc. Caio Castanho Xavier for Ti-15Zr-15Mo samples and Dr. Vânia Villas Bôas (INL) for her inestimable help in planning biological tests.

References

Afolaranmi, G.A., Akbar, M., Brewer, J., Grant, M.H., 2012. Distribution of metal released from cobalt-chromium alloy orthopaedic wear particles implanted into air pouches in mice. J. Biomed. Mater. Res. 100A, 1529–1538.

Alves, A.C., Oliveira, F., Wenger, F., Ponthiaux, P., Celis, J.P., Rocha, L.A., 2013. Tribocorrosion behaviour of anodic treated titanium surfaces intended for dental implants. J. Phys. D Appl. Phys. 46, 404001.

Alves, S.A., Saénz, R.B.V., Garcia, D.V.M.P., Igartua, A., Fernandes, M.H., Rocha, L.A., 2015. Tribocorrosion behavior of calcium- and phosphorous-enriched titanium oxide films and study of osteoblast interactions for dental implants. Bio. Tribo. Corros. 1, 1–21.

Amanatullah, D.F., Sucher, M.G., Bonadurer, G.F., Pereira, G.C., Taunton, M.J., 2016. Metal in total hip arthroplasty: wear particles, biology, and diagnosis. Orthopedics 39, 371–379.

Bezerra, F., Ferreira, M.R., Fontes, G.N., Fernandes, C.J.C., Andia, D.C., Cruz, N.C., Silva, R.A., Zambuzzi, W.F., 2017. Nano hydroxyapatite-blasted titanium surface affects pre-osteoblast morphology by modulating critical intracellular pathways. Biotechnol. Bioeng. 114, 1888–1898.

Bitar, D., Parvizi, J., 2015. Biological response to prosthetic debris. World J. Orthoped. 6, 172–189.

Chen, Q., Thouas, G.A., 2015. Metallic implant biomaterials. Mater. Sci. Eng. R Rep. 87, 1–57.

Cordeiro, J.M., Barão, V.A.R., 2017. Is there scientific evidence favoring the substitution of commercially pure titanium with titanium alloys for the manufacture of dental implants? Mater. Sci. Eng. C 71, 1201–1215.

Correa, D.R.N., Kuroda, P.A.B., Grandini, C.R., 2014. Structure, microstructure and selected mechanical properties of Ti-Zr-Mo alloys for biomedical applications. Adv. Mater. Res. 922, 75–80.

Correa, D.R.N., Kuroda, P.A.B., Grandini, C.R., Rocha, L.A., Oliveira, F.G.M., Alves, A.C., Toptan, F., 2016. Tribocorrosion behavior of β-type Ti-15Zr-based alloys. Mater. Lett. 179, 118–121.

Correa, D.R.N., Vicente, F.B., Araujo, R.O., Lourenço, M.L., Kuroda, P.A.B., Buzalaf, M.A.R., Grandini, C.R., 2015. Effect of the substitutional elements on the microstructure of the Ti-15Mo-Zr and Ti-15Zr-Mo systems alloys. J. Mater. Res. Technol. 4, 180–185.

Cvijović-Alagić, I., Cvijović, Z., Bajat, J., Rakin, M., 2016. Electrochemical behaviour of Ti-6Al-4V alloy with different microstructures in a simulated bio-environment. Mater. Corros. 67, 1075–1087.

Fernandes, C.J.C., Bezerra, F., Ferreira, M.R., Andrade, A.F.C., Pinto, T.S., Zambuzzi, W.F., 2018. Nano hydroxyapatite-blasted titanium surface creates a biointerface able to govern Src-dependent osteoblast metabolism as prerequisite to ECM remodeling. Colloids Surf. B Biointerfaces 163, 321–328.

Geetha, M., Singh, A.K., Asokamani, R., Gogia, A.K., 2009. Ti based biomaterials, the ultimate choice for orthopaedic implants - a review. Prog. Mater. Sci. 54, 397–425.

Gepreel, M.A.-H., Niinomi, M., 2013. Biocompatibility of Ti-alloys for long-term implantation. J. Mech. Behav. Biomed. Mater. 20, 407–415.

Hacisalihoglu, I., Samancioglu, A., Yildiz, F., Purcek, G., Alsaran, A., 2015. Tribocorrosion properties of different type titanium alloys in simulated body fluid. Wear 332–333, 679–686.

Haleem-Smith, H., Argintar, E., Bush, C., Hampton, D., Postma, W.F., Chen, F.H., Rimington, T., Lamb, J., Tuan, R.S., 2012. Biological responses of human mesenchymal stem cells to titanium wear debris particles. J. Orthop. Res. 30, 853–863.

Hallab, N.J., Jacobs, J.J., 2017. Chemokines associated with pathologic responses to orthopedic implant debris. Front. Endocrinol. (Lausanne). 8, 1–10.

Hallab, N.J., Mikecz, K., Vermes, C., Skipor, A., Jacobs, J.J., 2001. Orthopaedic implant related metal toxicity in terms of human lymphocyte reactivity to metal-protein complexes produced from cobalt-base and titanium-base implant alloy degradation. Mol. Cell. Biochem. 222, 127–136.

Hongtao, L., Shirong, G., Shoufan, C., Shibo, W., 2011. Comparison of wear debris generated from ultra high molecular weight polyethylene in vivo and in artificial joint simulator. Wear 271, 647–652.

Horev-Azaria, L., Kirkpatrick, C.J., Korenstein, R., Marche, P.N., Maimon, O., Ponti, J., Romano, R., Rossi, F., Golla-Schindler, U., Sommer, D., Uboldi, C., Unger, R.E., Villiers, C., 2011. Predictive toxicology of cobalt nanoparticles and ions: comparative in vitro study of different cellular models using methods of knowledge discovery from data. Toxicol. Sci. 122, 489–501.

Konttinen, Y.T., Pajarinen, J., 2013. Adverse reactions to metal-on-metal implants. Nat. Rev. Rheumatol. 9, 5–6.

Kumar, P., Nagarajan, A., Uchil, P.D., 2018. Analysis of cell viability by the MTT assay. Cold Spring Harb. Protoc. 2018 (6). https://doi.org/10.1101/pdb.prot095505.

Kwon, Y.-M., Xia, Z., Glyn-Jones, S., Beard, D., Gill, H.S., Murray, D.W., 2009. Dose-dependent cytotoxicity of clinically relevant cobalt nanoparticles and ions on macrophages in vitro. Biomed. Mater. 4, 025018.

Landgraeber, S., Jäger, M., Jacobs, J.J., Hallab, N.J., 2014. The pathology of orthopedic implant failure is mediated by innate immune system cytokines. Mediat. Inflamm. 185150.

Lee, S.-S., Sharma, A.R., Choi, B.-S., Jung, J.-S., Chang, J.-D., Park, S., Salvati, E.A., Purdue, E.P., Song, D.-K., Nam, J.-S., 2012. The effect of TNF-alpha secreted from macrophages activated by titanium particles on osteogenic activity regulated by WNT/BMP signaling in osteoprogenitor cells. Biomaterials 33, 4251–4263.

Li, X., Liu, W., Sun, L., Aifantis, K.E., Yu, B., Fan, Y., Feng, Q., Cui, F., Watari, F., 2014. Effects of physicochemical properties of nanomaterials on their toxicity. J. Biomed. Mater. Res. A 103, 2499–2507.

Li, Y., Boraschi, D., 2016. Endotoxin contamination: a key element in the interpretation of nanosafety studies. Nanomedicine 11, 269–287.

Madejczyk, M.S., Baer, C.E., Dennis, W.E., Minarchick, V.C., Leonard, S.S., Jackson, D.A., Stallings, J.D., Lewis, J.A., 2015. Temporal changes in rat liver gene expression after acute cadmium and chromium exposure. PLoS One 10, 1–27.

Magalhães, P.O., Lopes, A.M., Mazzola, P.G., Rangel-Yagui, C., Penna, T.C., Pessoa Jr, A., 2007. Methods of endotoxin removal from biological preparations: a review. J. Pharm. Pharm. Sci. 10, 388–404.

Mathew, M.T., Srinivasa Pai, P., Pourzal, R., Fischer, A., Wimmer, M.A., 2009. Significance of tribocorrosion in biomedical applications: overview and current status. Adv. Tribol. 2009https://doi.org/10.1155/2009/250986. 250986.

McIntyre, C.A., Reinin, G., 2009. Reduction in endotoxin levels after performing the prepare for aseptic sort procedure on the BD FACSAria II flow cytometer. BD Biosci. Appl. Note 12.

Monopoli, M.P., Walczyk, D., Campbell, A., Elia, G., Lynch, I., Baldelli Bombelli, F., Dawson, K.A., 2011. Physical-Chemical aspects of protein corona: relevance to in vitro and in vivo biological impacts of nanoparticles. J. Am. Chem. Soc. 133, 2525–2534.

Mostardi, R.A., Kovacik, M.W., Ramsier, R.D., Bender, E.T., Finefrock, J.M., Bear, T.F., Askew, M.J., 2010. A comparison of the effects of prosthetic and commercially pure metals on retrieved human fibroblasts: the role of surface elemental composition. Acta Biomater. 6, 702–707.

Niinomi, M., Nakai, M., Hieda, J., 2012. Development of new metallic alloys for biomedical applications. Acta Biomater. 8, 3888–3903.

Oliveira, C.A., Candelária, I.S., Oliveira, P.B., Figueiredo, A., Caseiro-Alves, F., 2015. Metallosis: a diagnosis not only in patients with metal-on-metal prostheses. Eur. J. Radiol. 2, 3–6.

Oliveira, F.G., Ribeiro, A.R., Perez, G., Archanjo, B.S., Gouvea, C.P., Araújo, J.R., Campos, A.P.C., Kuznetsov, A., Almeida, C.M., Maru, M.M., Achete, C.A., Ponthiaux, P., Celis, J.P., Rocha, L.A., 2015. Understanding growth mechanisms and tribocorrosion behaviour of porous TiO_2 anodic films containing calcium, phosphorous and magnesium. Appl. Surf. Sci. 341, 1–12.

Papageorgiou, I., Shadrick, V., Davis, S., Hails, L., Schins, R., Newson, R., Fisher, J., Ingham, E., Case, C.P., 2008. Macrophages detoxify the genotoxic and cytotoxic effects of surgical cobalt chrome alloy particles but not quartz particles on human cells in vitro. Mutat. Res. Fund Mol. Mech. Mutagen 643, 11–19.

Pederzoli, F., Tosi, G., Vandelli, M.A., Belletti, D., Forni, F., Ruozi, B., 2017. Protein corona and nanoparticles: how can we investigate on? Wiley Interdiscip. Rev. Nanomedicine Nanobiotechnology 9, e1467.

Perumal, G., Geetha, M., Asokamani, R., Alagumurthi, N., 2014. Wear studies on plasma sprayed Al_2O_3-40 wt% 8YSZ composite ceramic coating on Ti-6Al-4V alloy used for biomedical applications. Wear 311, 101–113.

Peruzzi, B., Cappariello, A., Del Fattore, A., Rucci, N., De Benedetti, F., Teti, A., 2012. C-Src and IL-6 inhibit osteoblast differentiation and integrate IGFBP5 signalling. Nat. Commun. 3, 610–630.

Ponthiaux, P., Wenger, F., Celis, J., 2012. Tribocorrosion : material behavior under combined conditions of corrosion and mechanical loading. In: Corrosion Resistance, pp. 81–106.

Pourzal, R., Catelas, I., Theissmann, R., Kaddick, C., Fischer, A., 2011. Characterization of wear particles generated from CoCrMo alloy under sliding wear conditions. Wear 271, 1658–1666.

Ribeiro, A.R., Gemini-Piperni, S., Travassos, R., Lemgruber, L., Silva, R.C., Rossi, A.L., Farina, M., Anselme, K., Shokuhfar, T., Shahbazian-Yassar, R., Borojevic, R., Rocha, L.A., Werckmann, J., Granjeiro, J.M., 2016. Trojan-like internalization of anatase titanium dioxide nanoparticles by human osteoblast cells. Sci. Rep. 6, 23615.

Rocha, S.S., Adabo, G.L., Henriques, G.E.P., Nóbilo, M.A.A., 2006. Vickers hardness of

cast commercially pure titanium and Ti-6Al-4V alloy submitted to heat treatments. Braz. Dent. J. 17, 126–129.
Rossi, M.C., Bezerra, F.J.B., Silva, R.A., Crulhas, B.P., Fernandes, C.J.C., Nascimento, A.S., Pedrosa, V.A., Padilha, P., Zambuzzi, W.F., 2017. Titanium-released from dental implant enhances pre-osteoblast adhesion by ROS modulating crucial intracellular pathways. J. Biomed. Mater. Res. 105 (Part A), 2968–2976.
Sansone, V., Pagani, D., Melato, M., 2013. The effects on bone cells of metal ions released from orthopaedic implants. A review. Clin. Cases Miner. Bone Metab. 10, 34–40.
Soto-Alvaredo, J., Blanco, E., Bettmer, J., Hevia, D., Sainz, R.M., López Chavés, C., Sánchez, C., Llopis, J., Sanz-Medel, A., Montes-Bayón, M., 2014. Evaluation of the biological effect of Ti generated debris from metal implants: ions and nanoparticles. Metallomics 6, 1702–1708.
Sukur, E., Akman, Y.E., Ozturkmen, Y., Kucukdurmaz, F., 2016. Particle Disease: a current review of the biological mechanisms in periprosthetic osteolysis after hip arthroplasty. Open Orthop. J. 10, 241–251.
Sundell, G., Dahlin, C., Andersson, M., Thuvander, M., 2017. The bone-implant interface of dental implants in humans on the atomic scale. Acta Biomater. 48, 445–450.
Vasconcelos, D.M., Santos, S.G., Lamghari, M., Barbosa, M.A., 2016. The two faces of metal ions: from implants rejection to tissue repair/regeneration. Biomaterials 84, 262–275.
Veronesi, F., Tschon, M., Fini, M., 2017. Gene expression in osteolysis: review on the identification of altered molecular pathways in preclinical and clinical studies. Int. J. Mol. Sci. 18, 499–522.
Wang, S., Ge, S., Liu, H., Huang, X., 2010. Wear behaviour and wear debris characterization of UHMWPE on alumina ceramic, stainless steel, CoCrMo and Ti6Al4V hip prostheses in a hip joint simulator. J. Biomimetics, Biomaterials Tissue Eng. 7, 7–25.
Wang, Z.B., Hu, H.X., Zheng, Y.G., Ke, W., Qiao, Y.X., 2016. Comparison of the corrosion behavior of pure titanium and its alloys in fluoride-containing sulfuric acid. Corros. Sci. 103, 50–65.
Watters, T.S., Cardona, D.M., Menon, K.S., Vinson, E.N., Bolognesi, M.P., Dodd, L.G., 2010. Aseptic lymphocyte-dominated vasculitis-associated lesion: a clinicopathologic review of an underrecognized cause of prosthetic failure. Am. J. Clin. Pathol. 134, 886–893.
Wu, J., Yin, G., Chen, H.-Q., Sung, K.-L.-P., 2008. The influence of titanium particles size on bone marrow mensenchymal stem cells viability. Key Eng. Mater. 361–363 (II), 1063–1066.
Xavier, C.C., Correa, D.R.N., Grandini, C.R., Rocha, L.A., 2017. Low temperature heat treatments on Ti-15Zr-xMo alloys. J. Alloy. Comp. 727, 246–253.
Zhang, D., Wong, C.S., Wen, C., Li, Y., 2017. Cellular responses of osteoblast-like cells to 17 elemental metals. J. Biomed. Mater. Res. A 105, 148–158.